NOAA Technical Memorandum ERL ETL-286

AUTOMATED EDITING OF SPECTRA FROM WIND PROFILERS

E.E. Gossard

Environmental Technology Laboratory
Boulder, Colorado
December 1997

noaa NATIONAL OCEANIC AND ATMOSPHERIC ADMINISTRATION / Environmental Research Laboratories

NOAA Technical Memorandum ERL ETL-286

AUTOMATED EDITING OF SPECTRA FROM WIND PROFILERS

Earl E. Gossard

Environmental Technology Laboratory
Boulder, Colorado
December 1997

c.2

UNITED STATES DEPARTMENT OF COMMERCE

William M. Daley
Secretary

NATIONAL OCEANIC AND ATMOSPHERIC ADMINISTRATION

D. JAMES BAKER
Under Secretary for Oceans and Atmosphere/Administrator

Environmental Research Laboratories

James L. Rasmussen
Director

NOTICE

Mention of a commercial company or product does not constitute an endorsement by the NOAA Environmental Research Laboratories. Use of information from this publication concerning proprietary products or the test of such products for publicity or advertising purposes is not authorized.

For sale by the National Technical Information Service, 5285 Port Royal Road
Springfield, VA 22061

Contents

Automated Editing of Spectra from Wind Profilers

by

Earl E. Gossard
Science and Technology Corporation/ETL/NOAA
Boulder, CO 80303

Abstract. This report describes a procedure for editing complicated Doppler spectra observed by radar wind profilers. A fundamental assumption is that the atmospheric backscatter is more highly correlated between opposing beams and between successive cycles than are spurious targets such as aircraft, cars and birds. It is assumed that the profiler cycles through five beams and that full spectra are available for processing. Cross correlation functions of the spectra from opposing radials and from successive cycles of vertical beams are calculated and used to choose the desired peak produced by atmospheric return. Spectral peaks that are unreasonably strong to be atmospheric backscatter are flagged, and peaks that indicate movement that is unreasonably rapid are rejected. Images at the same plus and minus velocities are rejected if they are of comparable magnitude, and the image rejection technique, coupled with the cross-correlation analysis, is used to reject stationary clutter. The procedure also uses persistence in time and continuity in height. It accepts only spectral peaks that lie within a velocity window from that of the preceding selected peak..

Introduction

Past efforts to use 0 and 2nd moments of spectra collected by wind profilers such as those described by Gossard et al (1990) have been largely unsuccessful and have discouraged applications of wind profilers for retrieving profiles of properties other than wind speed and direction. Post-experiment analysis has revealed that the failure of early efforts was related to two factors: 1) Moments of the spectra, rather than the spectra, were edited and used. Raw spectra were not, in fact, available, and subsequent studies have shown the spectra (collected near Stapleton Airport) to be very "noisy". 2) The earlier experiments were carried out in a locality where substantial humidity gradients were rare except during frontal passages when clouds and rain contaminated the (915 MHz) radar data. (The radars, in fact, proved to be good cloud research tools.)

The goal of this report is to describe a technique for editing profiler Doppler spectra rather than editing the moment data. Specifically, we reject spurious spectral peaks due to:

1) unwanted moving targets (such as aircraft and birds, as in the Pt. Loma data),

2) unwanted image peaks in the spectra from whatever source (especially prominent in theVandenburg and Pt. Loma data),
3) ground clutter which was especially confusing in the Vandenburg data).

The criteria for rejection of non-atmospheric return from noisy spectra were:

1) rejection of targets that exceed atmospherically reasonable backscatter ($C_N^2 > 5x10^{-2}$). (This is implemented as a flag in this software.)
2) rejection of targets that exceed atmospherically reasonable radial speeds (6 m s^{-2}).
3) suppression of targets that are not highly correlated on opposing radial beams.
4) suppression of targets that are not highly correlated from cycle to cycle (a kind of spectral consensus)
5) Rejection of images when their magnitude lies within a factor of 5 of each other.
6) Rejection of ground clutter by a correlation technique that suppresses stationary objects.

In these software procedures we assume we have the redundancy of a 5-beam system; that is, one vertical beam and four off-vertical beams, pairs of which are azimuthally directed 180 deg from each other. We also assume we are given "raw" spectra. We note that opposing beams would not necessarily lead to the same horizontal wind even if they were simultaneous, because calculation of the horizontal wind from an off-vertical radial includes a vertical velocity contribution that adds positively to one radial but subtracts from the other. In fact we use the lagged cross correlation function between opposing radials to calculate the vertical velocity.

An Approach to Spectral Peak Selection

An example of the contamination of profiler Doppler spectra that can occur is shown in Fig. 1. This is a good case against which it is recommended that all spectral editing techniques be tested. This output is from the Profiler On-line Program (POP) developed by NOAA's Aeronomy Laboratory. It shows stacked spectra of the four off-vertical beams. On each spectrum the moment data are displayed as a + (1^{st} moment) with a horizontal bar through the cross (2^{nd} moment). We see that without sophisticated peak selection the moment data can be very unrealistic in the lower range gates where aircraft and bird contamination are severe so we next consider criteria for selection of the atmospheric spectral peaks.

Signal strength and velocity constraints - We first place limitations on the acceptable backscattered power and speed of movement of atmospheric targets. We calculate the C_N^2 spectral density and compare the magnitude of the peaks with what is expected from atmospheric backscatter. If the integrated C_N^2 under the peak is greater than $5x10^{-2}$ it is assumed that the signal is too large to be atmospheric and is rejected (flagged) as an artifact. We reject spectral elements the radial velocity of which is too high to be real air motion.

Off-vertical beams - In order to reject spurious artifacts such as aircraft and birds in the spectrum, the method assumes that spectra of natural atmospheric backscatter will be well correlated on opposing radial beams and will tend to persist in time. Therefore, the cross-correlation function between opposing pairs of radials is calculated, and the spectral lag for maximum correlation is

found. Because the wind is toward the radar on one radial and away from the radar on the other, one of the spectra must be reversed (i.e. the velocity axis changed in sign) before the correlation function is computed. An example of the stacked correlation functions is shown in Fig. 2. Assuming horizontal atmospheric uniformity over the profiler's beam sweeps, the vertical velocity can be calculated from the correlation lags. Using that vertical velocity, the spectra of the horizontal winds are calculated and their cross product taken, suitably lagged for maximum correlation. Spectral peaks that exist in one record but not in the other will have a zero (or very small) cross-product, while peaks that match in both records will have a large cross-product. Therefore the highest peak in the product spectrum is assumed to be the atmospheric contribution that is sought and that peak must be found by some software technique. Because of limited memory in our system, we use a procedure of first finding the spectral peaks. then the peaks of the peaks, then the peaks of the peaks of the peaks until two or less highest peaks remain. Then a simple logic statement provides the highest peak. Having the desired peak it is now necessary to get the bounds on the peak automatically. The bounds are found automatically from the second derivative of the spectrum with respect to velocity and choosing those innermost values that bracket the chosen peak. The procedure is shown schematically in Fig. 3. Examples of the peak selection achieved by this method for the case of Figure 1 are shown in Figs. 4 and 5 which are to be compared with the POP outputs in Fig. 1. The bounds are shown as dashed lines and the vertical velocity deduced from the cross-correlation is shown at the right, displaced by 5 ms^{-1} for clarity.

Clutter - The suppression of stationary clutter is conveniently achieved as a subset of the correlation analysis. The opposite shift in the spectra of the opposing beams that results from the correlation analysis causes the stationary (clutter) peaks to be split. This split provides a convenient criterion for clutter rejection through use of the image peak rejection software described above. Examples are shown in Figs. 6 and 7 where prominent clutter is found near zero at several heights. The POP results are shown on the left and the split peak method is shown on the right. The peak selection from POP does quite well in this case. It uses an algorithm based on continuity in height to track the peak from some pre-selected height that is uncontaminated. We have added the continuit feature to the clutter/image rejection algorithm described above and its performance is improved. For example, without persistency the wrong peak would have been selected at Gate 9 of Fig.7.

Images - Especially in the lower range gates, prominent spectral peaks are often found that are images of each other; that is, they are symmetrically located on the velocity axis at plus and minus velocities. These peaks are usually a contaminant to be ignored in the atmospheric peak selection. This can be done fairly simply, but it must be remembered that real atmospheric peaks also create images if co- and quadrature components are not properly balanced out in the receiver system. Such peaks are real, and they obviously cannot be ignored. Therefore, criteria must be inserted in the softwarethat enables us to judge when the images should be ignored.. The suppression of these images is evident in Figs. 6 and 7. The lowest range gate has been ignored in our analysis because it is too severely contaminated to be useful.

Vertical Beam - The analysis of the vertical beam is essentially the same as the correlation

analysis of the off-vertical beams except that the velocity axis is not reversed on either of the cross-correlated spectra. The correlation then represents the persistency of the target with time and is roughly the equivalent of a consensus in the spectral domain (i. e.transient targets will be poorly correlated between successive sweep cycles of the profiler.) An example of the vertical beams corresponding to Figs. 4 and 5 is shown in Figs. 8.

Moment Calculations

Background - Historically wind profilers have been used mainly for 1st moment information; i. e. the radial wind components from which wind profiles can be calculated. For this purpose it has been economical to calculate total moments, then edit the moments by throwing away outliers in an orderly way; that is, by some kind of consensus test. This has generally worked well for fairly long consensuses (30 minutes to one hour). However, that method is poorly suited to the analysis of the short data samples used for comparison with balloon soundings, and it is not generally appropriate for 0-moment or 2nd moment analyses where the moments are sensitive to the shape and bounds of individual spectral peaks. Therefore, after the spectral editing described above, which finds the desired "peak", the problem remains to obtain the best possible 0 and 2nd moments even when the appropriate peak is not isolated from other extraneous peaks. In fact, the selected peak may often be overlapped by other peaks. Bounds and noise thresholds can then be important obstacles and some techniques have attempted to use criteria based on noise level and depth of the troughs between peaks. With real spectra we have generally found these techniques to be too poorly defined to be of much use.

Moments from Least-Squares Fit - A technique that is minimally sensitive to bounds and noise threshold has been described by Gossard et al. (1994,1997) for the extraction of 2nd moments of cloud spectra, and it is found also to work well with "clear-air" spectra (Gossard et al.1998). It assumes (Labbitt, 1981) that atmospheric Bragg-scatter spectra are Gaussian in shape. In this method a regression fit of the spectral points to a Gaussian between selected bounds is carried out on a Log S vs velocity squared plot and the 2nd moment is calculated from the slope of the regression line. Thus, if the spectral density of C_N^2 is given by the Gaussian function

$$S = S_0 \exp\left[-(w^2/2\,\sigma_w^2)\right] ,$$

it can be written logarithmically as an equation linear in w^2 , i. e.,

$$\lg S = \lg S_0 - [(2)(2.3026)\,\sigma_w^2]^{-1}\, w^2 ,$$

where S is the magnitude of C_N^2 spectral density and w is, for example, the vertical component of velocity. This method does not depend on integrating between bounds nor does it require a noise threshold selection. In fact, the only constraint imposed by bounds is to ensure that the selected points do not include points from adjacent, unwanted peaks. An early example of the techniqwe, used to get 2nd moments of cloud spectra is shown in Fig. 9 and clear-air examples from the Pt. Loma data are shown in Fig. 10.

Selecting the Bounds - In Fig. 3 a schematic spectrum was shown that illustrates the problem of selecting bounds when the spectral peaks overlap. We have found that the simplest and most robust method of bound selection is to find the points of maximum positive curvature (2nd derivative) in the spectrum and then to choose the pair of maxima that bracket the peak chosen. The spectrum from gate 7 in Fig. 7 illustrates the effectiveness of this bounds- selection technique for dealing with split peaks and for isolating the proper segments of the peak selected.

Conclusions

In spite of the many constraints described in this report, it is anticipated that the spectral peak chosen will occasionally fail; that is, it will disagree with human judgment in about 1 spectrum out of 100 in noisy data. Therefore, it is recommended that the software implemented include a near-real-time display of results superimposed on raw spectra with provision for human intervention to modify the occasional "bad" choise.

REFERENCES

Gossard, E. E., 1994. Measurement of cloud droplet spectra by Doppler radar. *J. Atmos. Oceanic Technol.*, 3:712–726.

Gossard, E. E., D. C. Welsh and R. G. Strauch, 1990. Radar-measured height profiles of C_n^2 and turbulent dissipation rate compared with radiosonde data during October 1989 at Denver. NOAA Technical Report ERL-442-WPL 63. 115 pp.

Gossard, E. E., J. B. Snider, E. E. Clothiaux, B. Martner, J. S. Gibson, R. A. Kropfli, and A. S. Frisch, 1997: The potential of 8-mm radars for remotely sensing cloud drop size distributions. *J. Atmos. Ocean. Technol.*, **14**, 76-87.

Gossard, E. E. , D. E. Wolfe, K. E. Moran, R. A. Paulus, K. D. Anderson and L. T. Rogers, 1998: Measurement of Clear-air Gradients and Turbulence Properties with Radar Wind Profilers. *J. Atmos. and Ocean. Technol. (in press)*

Labbitt, M., 1981: Coordinated radar and aircraft observations of turbulence. Rep. ATC–108, MIT Lincoln Laboratory, Cambridge, MA, 40 pp.

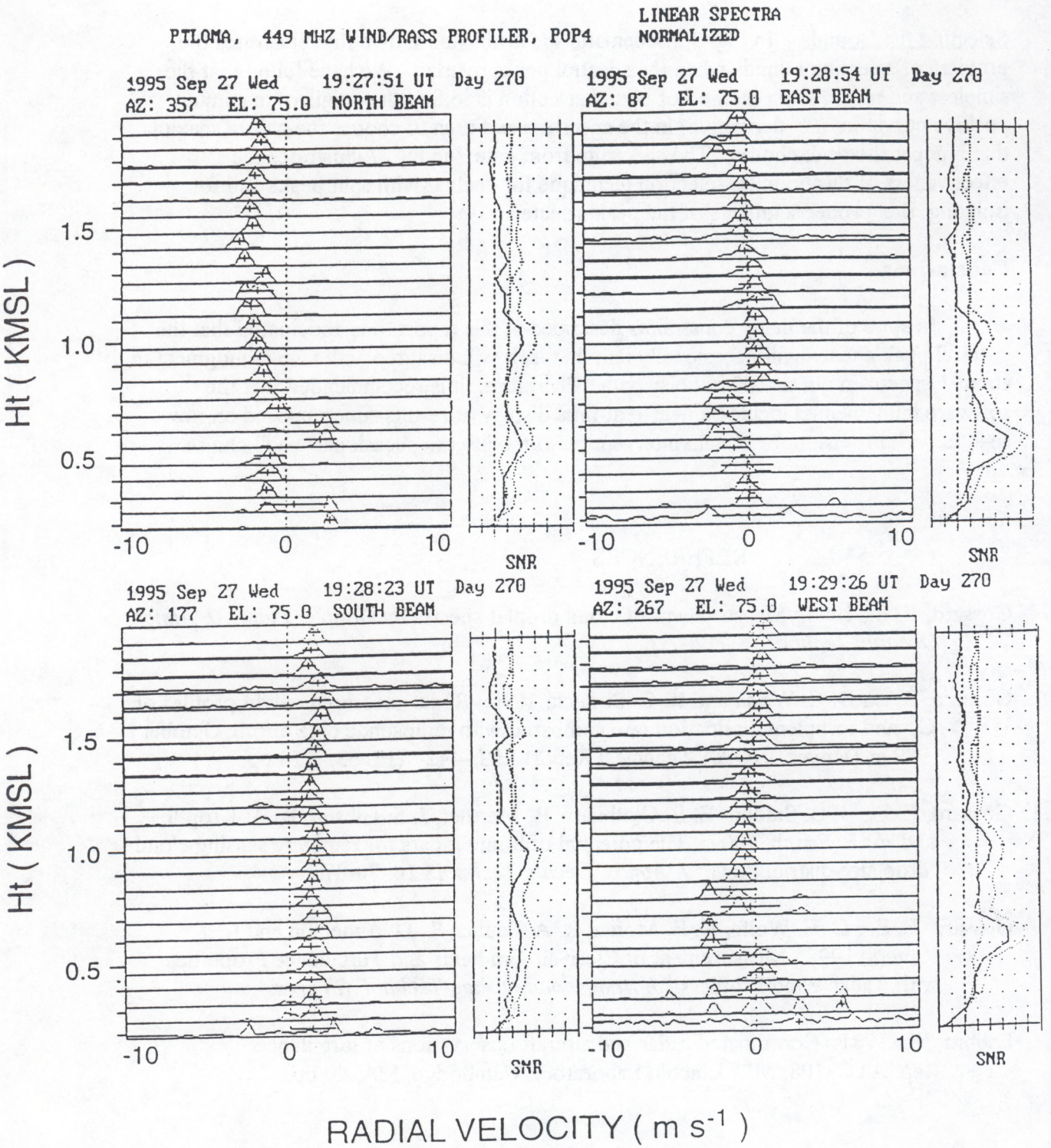

Fig. 1. Sample stacked spectra output from POP for the four beams that are 15 deg. off-vertical illustrated the contamination of profiler spectra from aircraft, birds, cars and probably insects.

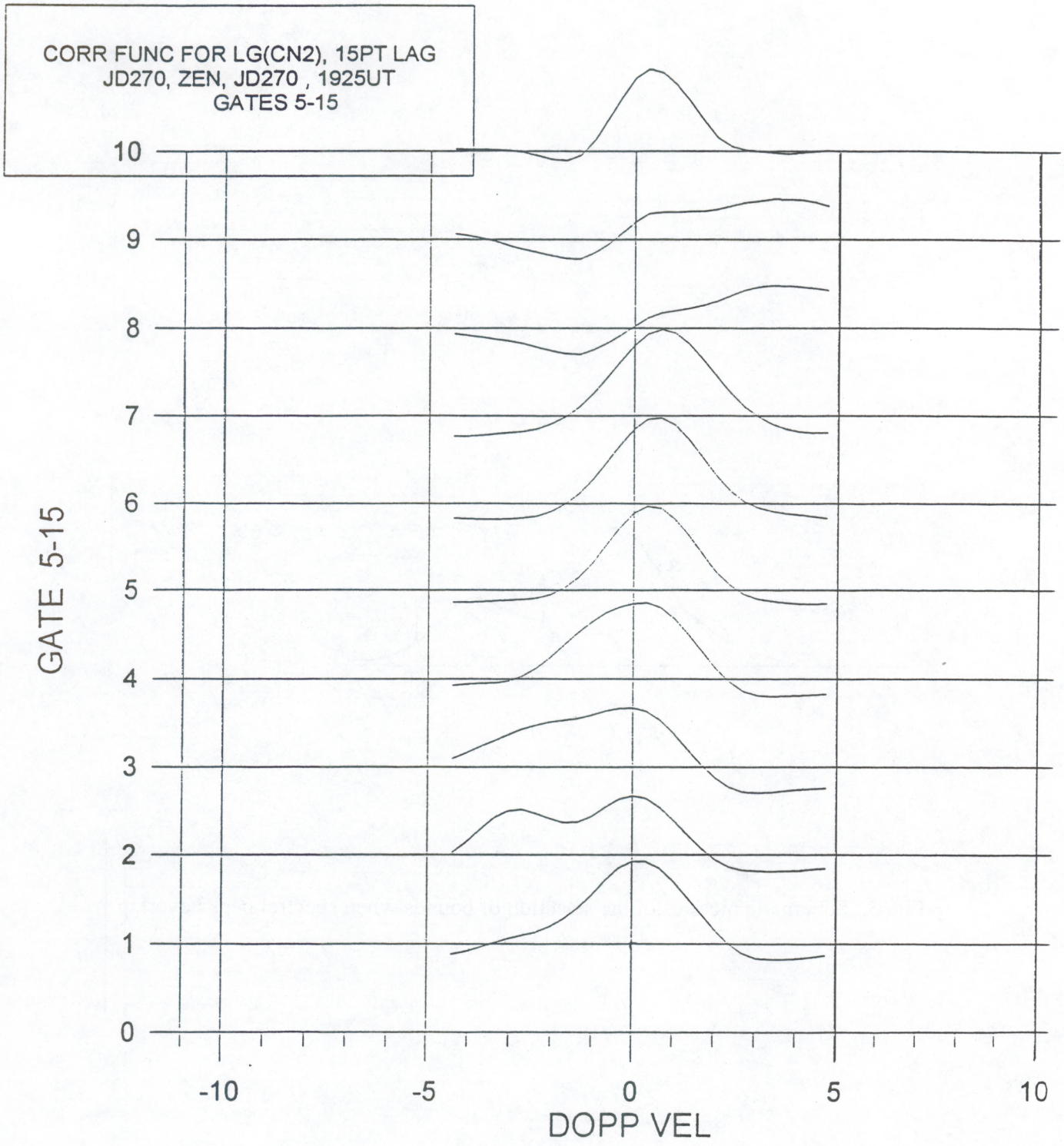

Fig. 2. Sample of stacked correlation functions found from cross correlating C_N^2 spectra from successive sweeps of the zenith beam.

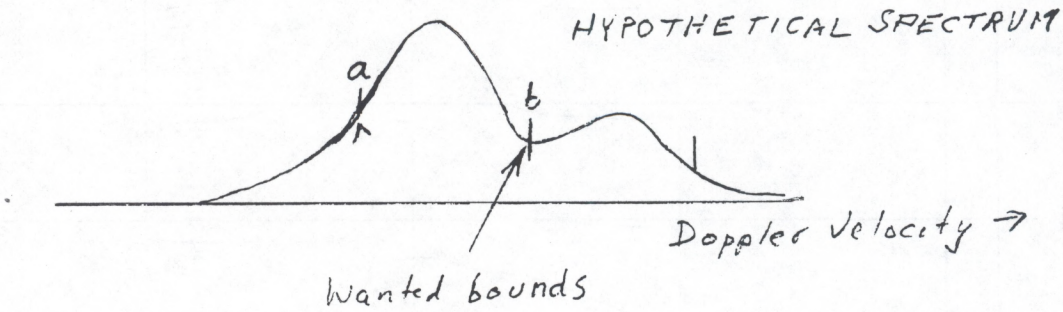

Fig. 3. Schematic pictures of the selection of bounds when spectral peaks overlap.

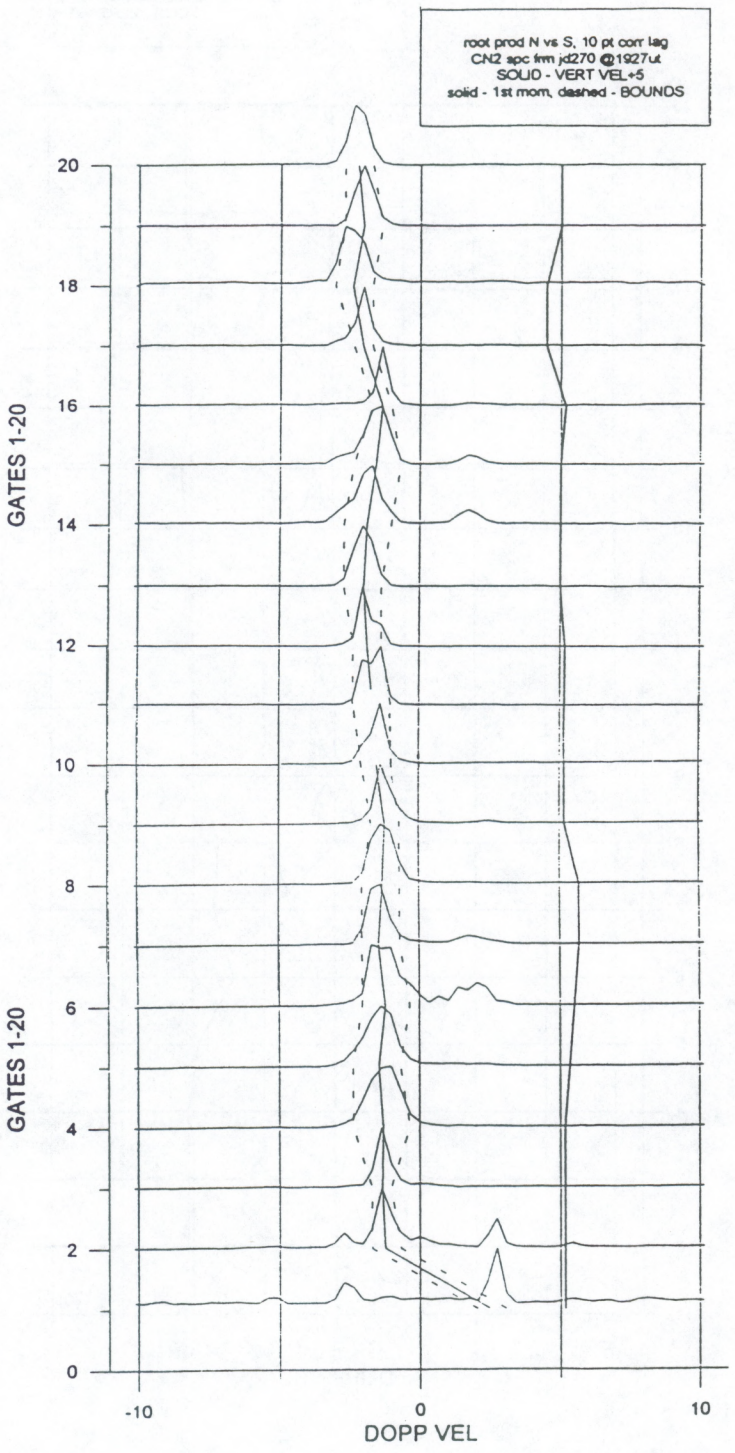

Fig. 4. Root of the cross product of N/S beam spectra that have been lagged for optimum correlation. Compare peak selection with Fig. 1. Solid profile on the right is vertical velocity shifted by 5 units. Bounds about selected peaks are shown as dashed profiles. See Fig. 3.

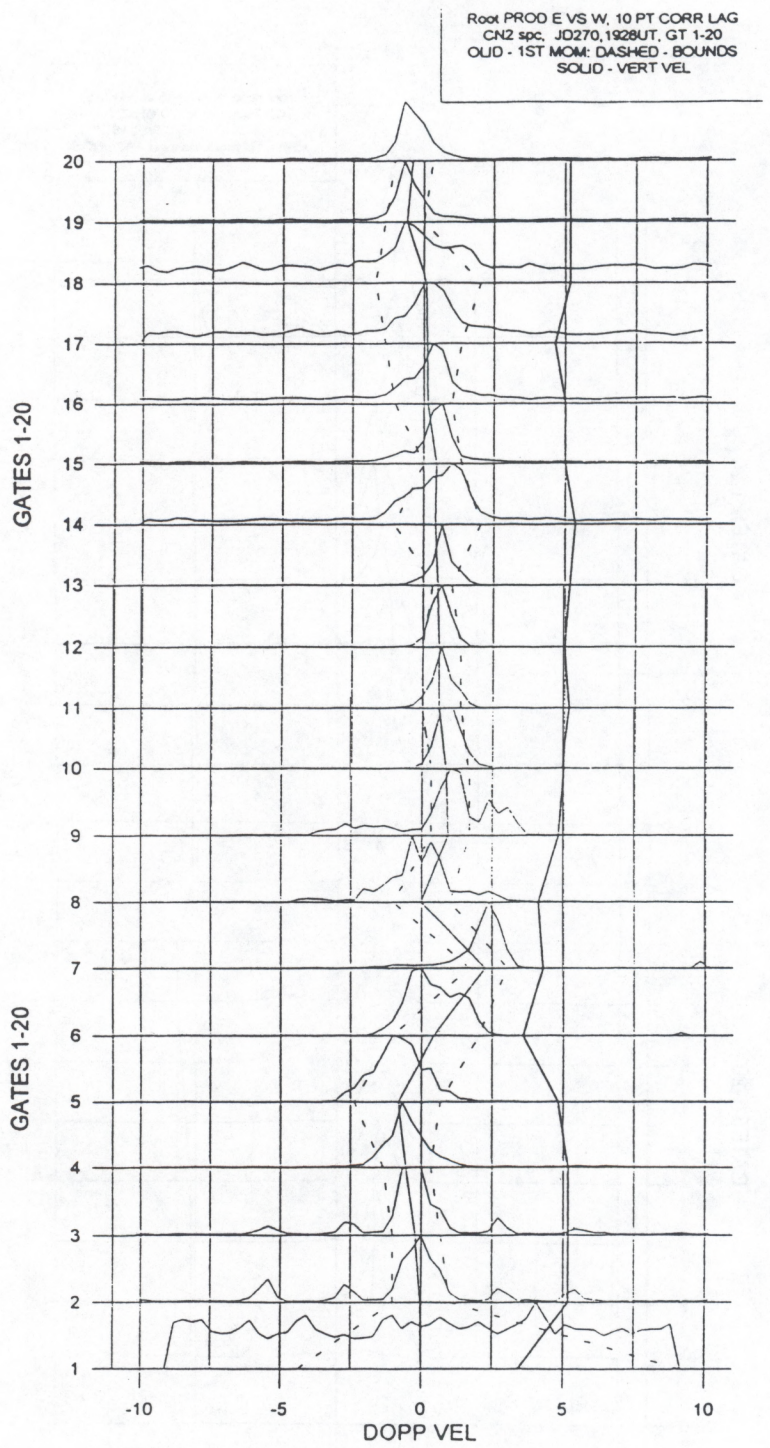

Fig. 5. Roots of the cross product of E/W beam spectra that have been lagged for optimum correlation. Compare peaks with display in Fig. 1. Solid profile on the right is vertical velocity shifted by 5 units. Peak selection and bounds found from the methods of this report are shown dashed.

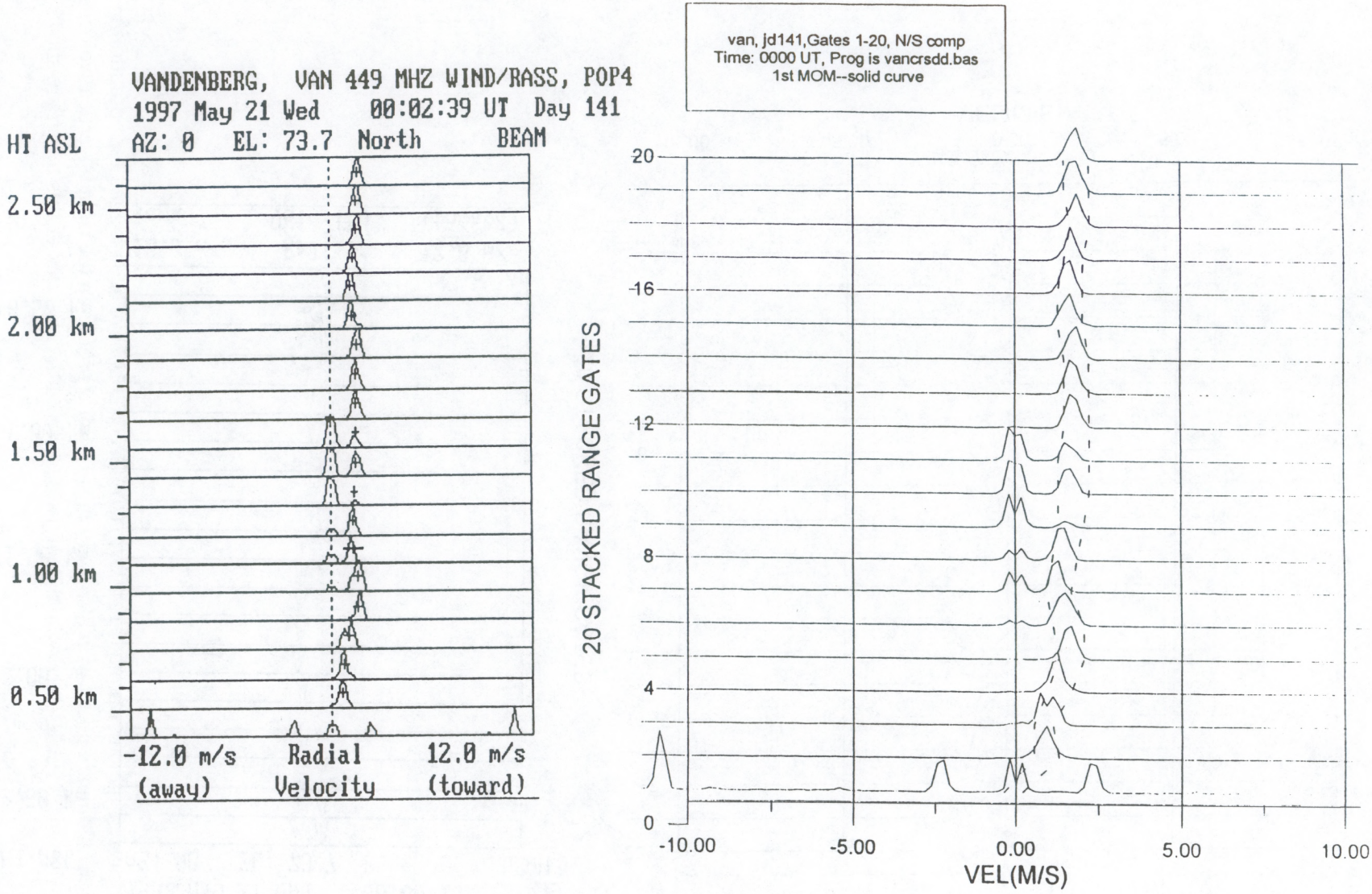

Fig. 6. Left: Sample POP display of stacked spectra for N component having severe clutter contamination near zero velocity. Right: Selected peaks and bounds found from the N/S beams fusing the clutter and image rejection of this report.

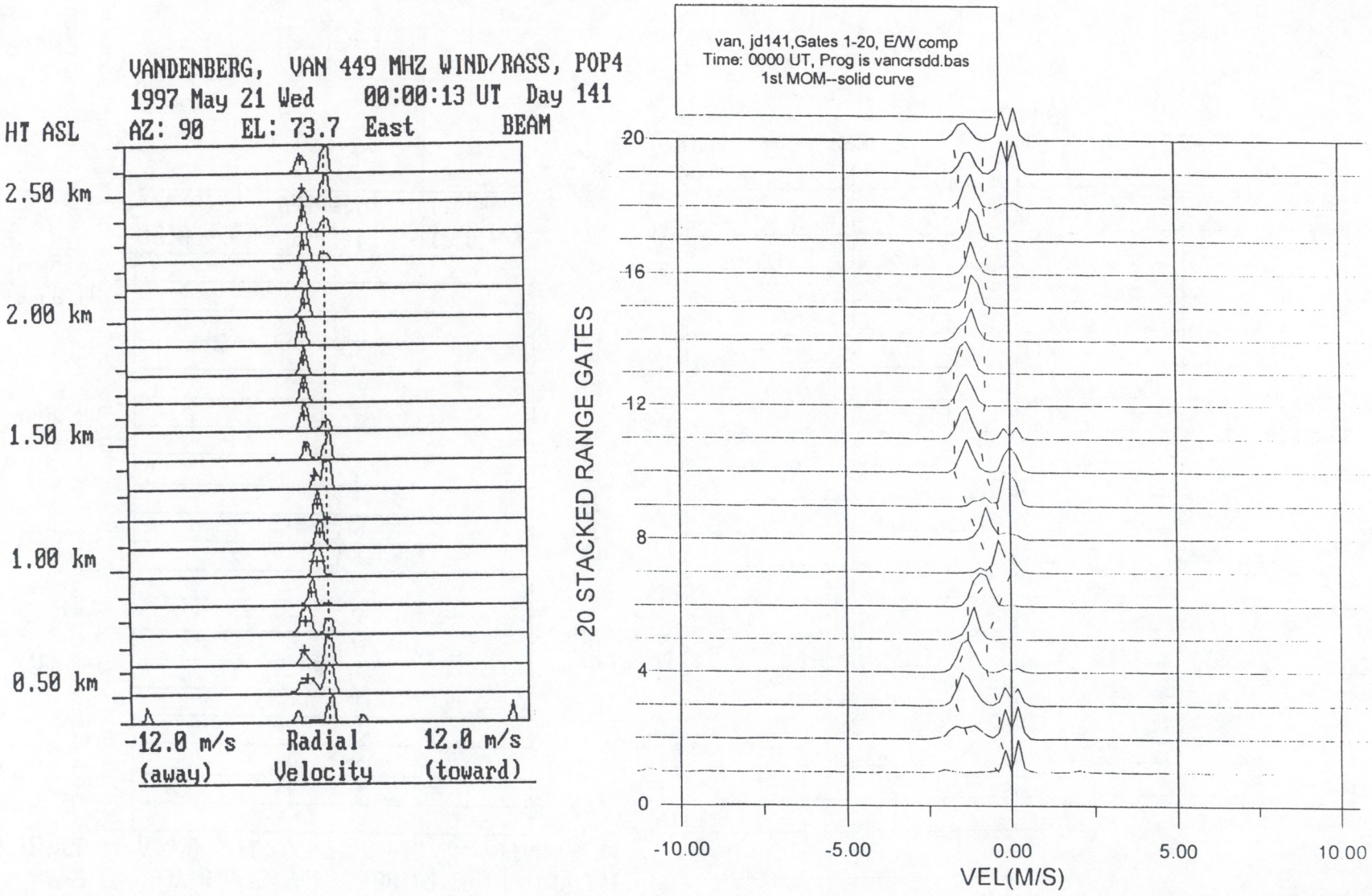

Fig. 7. Same as Fig. 6 but for the E/W beams.

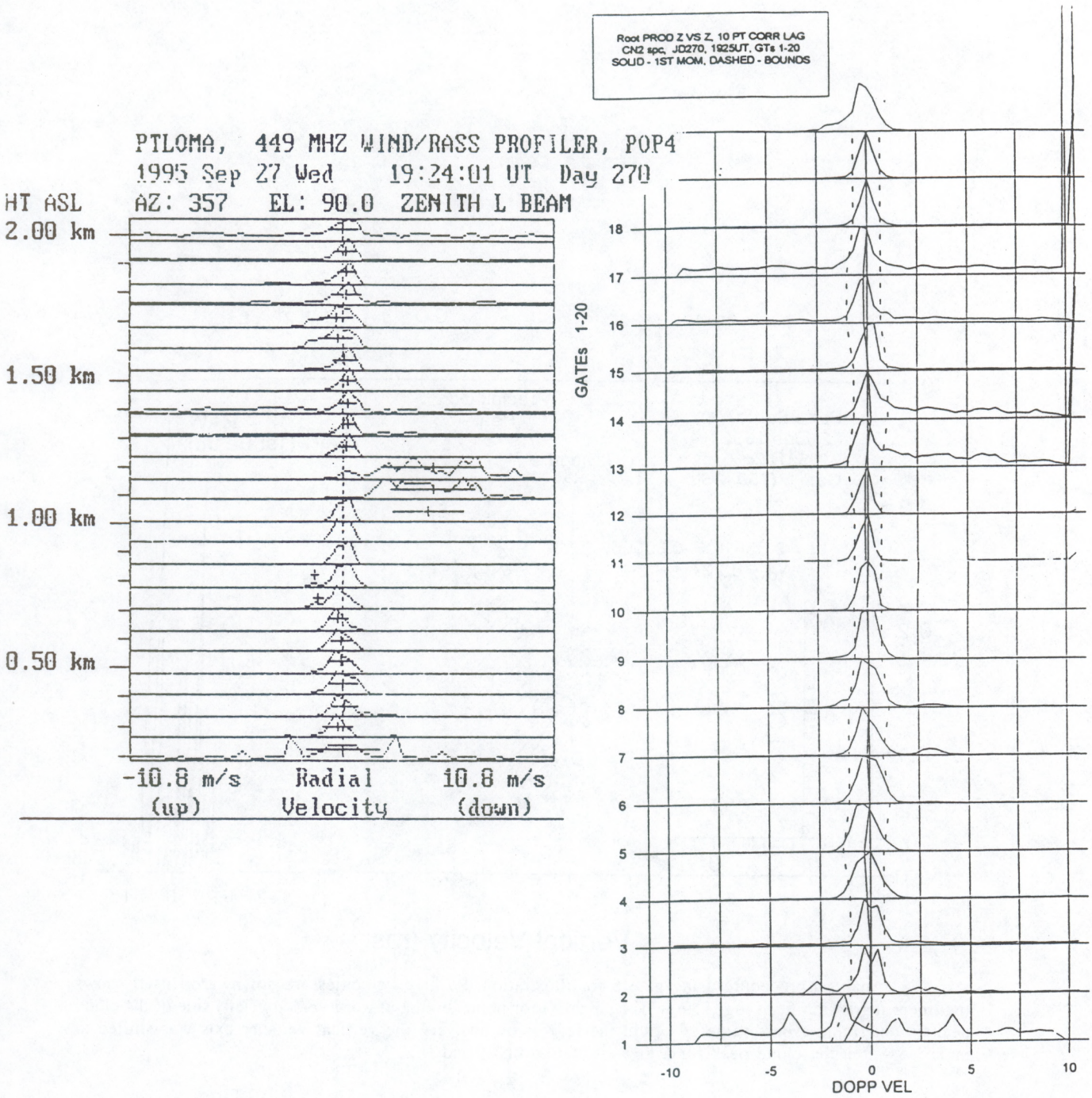

Fig. 8. Left: Sample POP display of stacked spectra showing much clutter, e.g. at gate 1 (a flock of birds?). Right: The root product peaks and bounds found from the cross correlation of successive beam sweeps.

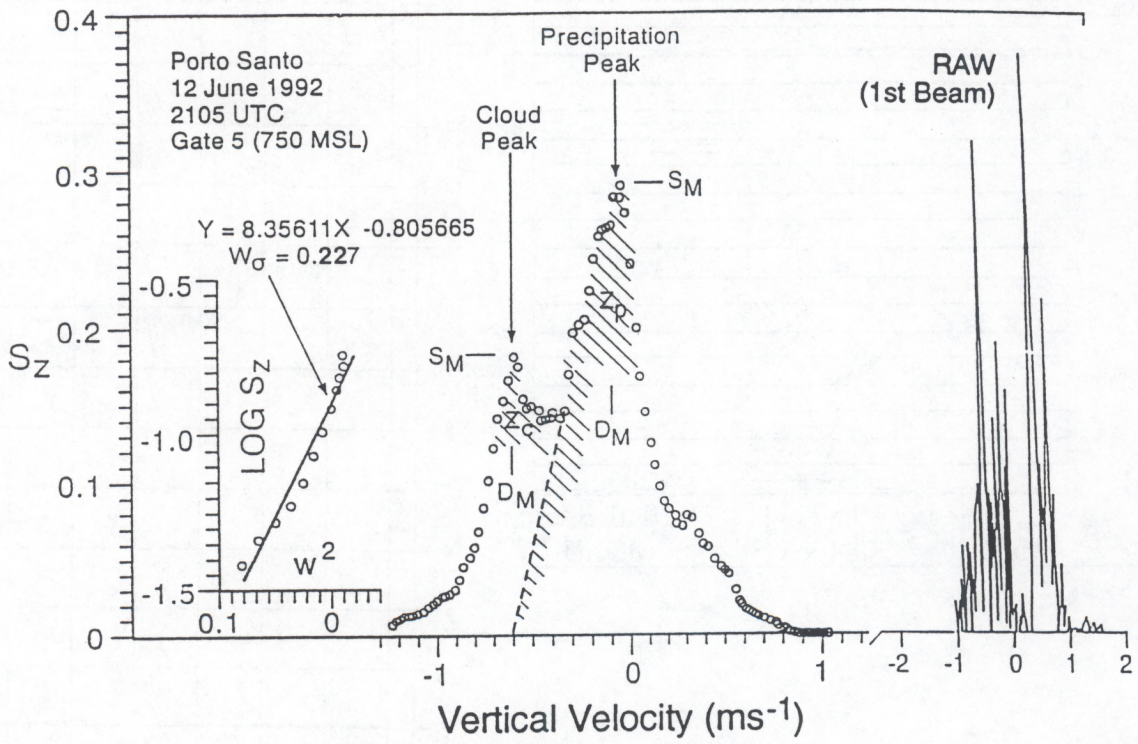

Analysis procedure using gate 5 for illustration. Positive velocities are downward. Insert shows the linear regression fit of $\log_{10}S_z$ to w^2 (i.e., Y vs X) for points on the upward velocity (left) side of the cloud peak to determine a best value of w_σ. In the regression analysis, the vertical velocity axis was shifted to make $w = 0$ at the cloud peak for a first estimation of w_σ and D_M.

Fig. 9. Cloud spectra recorded with an 8-mm radar illustrating the method of 2nd moment extraction from least square fitting of spectral data to a Gaussian function (see insert at left). (Original caption retained for further clarification).

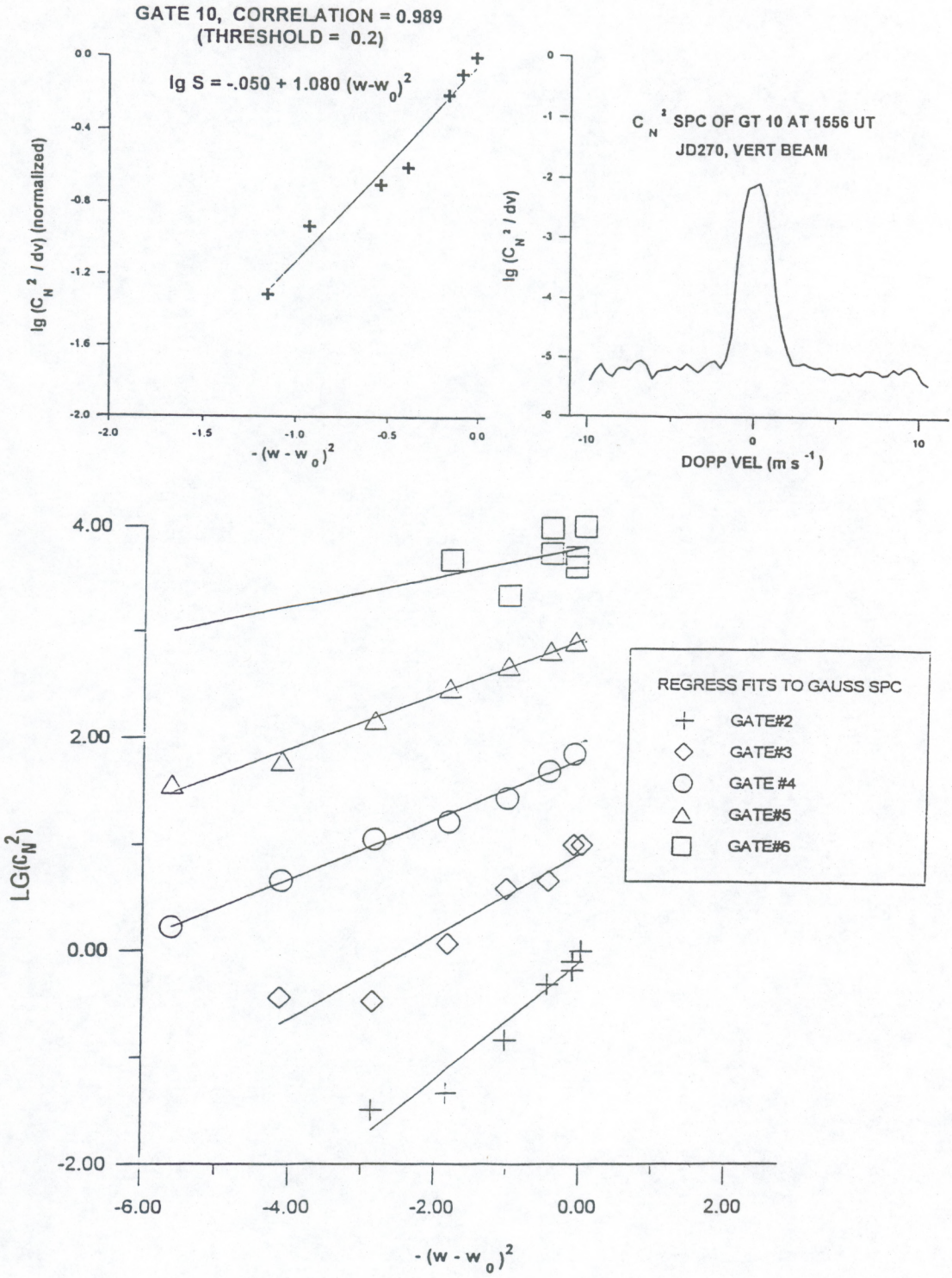

Fig. 10. Further illustration of least-square method of 2nd moment calculation.
Top: Method applied to gate 10 of Fig. 8.
Bottom: Sample of regression fits for other gates.

*U.S. GOVERNMENT PRINTING OFFICE 1998-0-673-018/40078